Supplemental Material

1. Additional characterization of the three E=I balance state crossings.

We have calculated distributions of mean interspike intervals (ISI) and their coefficients of variation (CV-ISIs) at the three crossings, to look at the spread of the network overall activity (Fig. S1). The distribution of CV-ISIs is the widest for first crossing. Note also that there are a large number of neurons that do not spike at all and hence the statistics in terms of neuron number is much lower. At second and third crossing most of the neurons are active and CV also declines. Relative increase in CV for the third crossing (as compared to the second one) is mostly driven by fact that the mean ISI is significantly smaller.

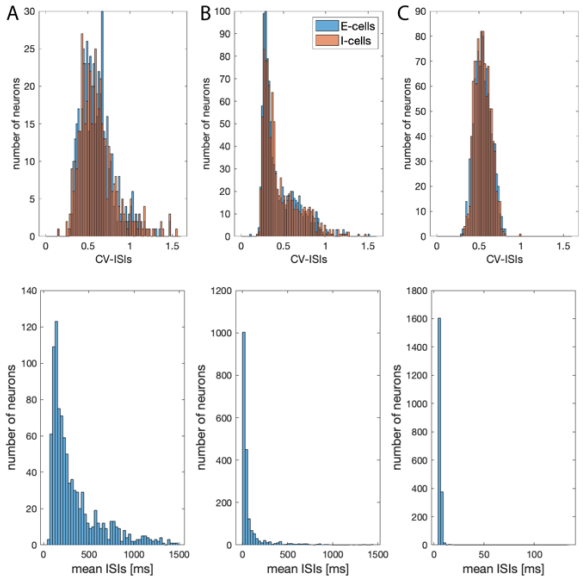

Fig S1. Distributions of coefficients of variation of interspike intervals (CV-ISIs; top) and distributions of mean neuronal ISI (bottom) for: A) first crossing; B) Second crossing and C) third crossing.

2. Detailed dynamics at the E=I balanced states: comparison of dynamics of firing frequency difference, voltage difference and net current difference at the three balanced states for different w_E values and noise frequency.

Near each of the three crossings of the E=I, we chose a value of w_E (blue, black and yellow data in Fig. S2) and increased E cells' noise frequency to vary the E/I ratio (similarly as on Fig. 6 of the main manuscript for one w_E value). For each w_E value, we examined the trajectory of the E/I ratio and the difference in firing rates between E and I cells (first column Fig. S2), and the difference between the absolute value of the mean membrane potentials of E and I cells (second column, Fig S2). Finally, we also assessed the trajectory of the E/I ratio vs. net current difference (third column, Fig S2; and vs. total current (E-I) in the network (fourth column, Fig. S2). Arrows indicate the direction of change as noise frequency increases. Changes due to increasing noise frequency follow the same path as those due to increasing w_E, indicating a qualitative consistency of effects (Fig. S2d, h, l).

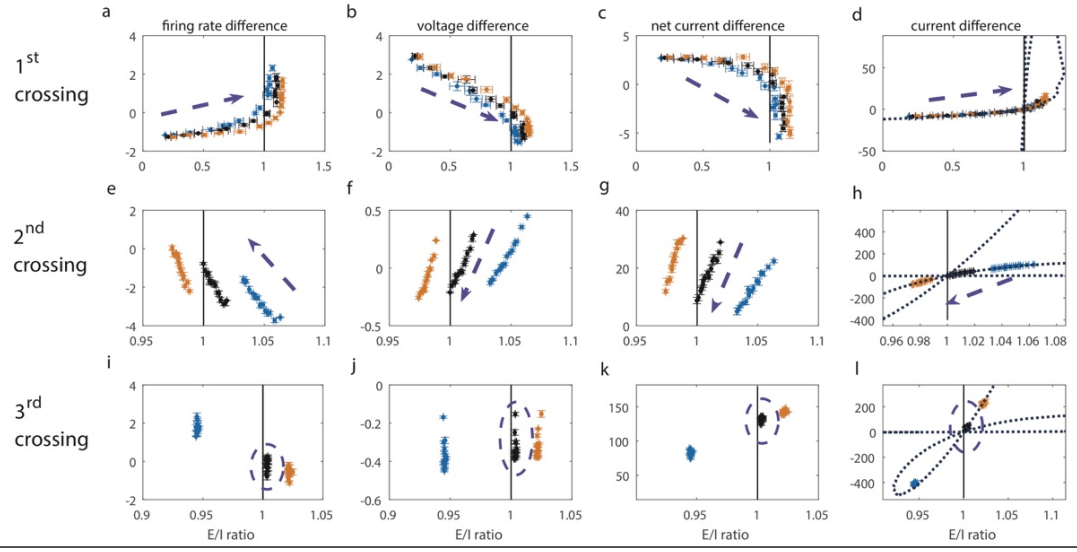

Figure S2. Comparison of network dynamics at the first (top row), second (middle row) and third (bottom row) crossings of the E=I balanced state. Near each E=I balanced state, three different values of w_E are chosen representing low (blue data points), medium (black data points) and high (yellow data points) values of w_E. For each value of w_E, the frequency of noise events to the E cells is varied between 5 and 75Hz while the noise event frequency to the I cells is kept at 40Hz (dashed arrows indicate direction of change with increasing noise frequency). Trajectories of E/I ratio values and (a, e, i) firing frequency difference between the E and I cells; (b, f, j) absolute value of mean voltage difference between the E and I cells; (c, g, k) "net current difference" (see text for description) between the E and I cells; and (d, h, l) total current (E-I).

3. Changes between the total synaptic current and E/I ratio relationship as a function of noise frequency.

The results presented in the manuscript pertain to the case when the external noise, in the form of a random kick, has average frequency of 40 Hz. We investigated additional noise frequencies set to 10Hz, 80Hz, and 120Hz. These results are presented in Fig. S3. We found that varying the noise frequency did not qualitatively change the relationship between the total synaptic current and E/I ratio, as it had only limited effects on loop sizes.

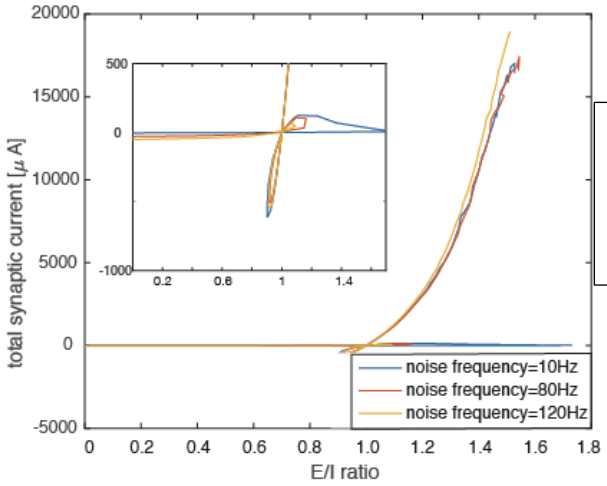

Figure S3. Changes in the total synaptic current/ E/I ratio in presence of different nose levels. The results are largely invariant to the noise frequency

4. Network wide E-I balance calculated for different cell models.

To exclude the possibility that the results are due to the unique properties of the modified Hodgkin-Huxley model we described in the main manuscript, we performed similar simulations for networks composed of different neuron models, in particular the Wang-Buzaki Model (WBM) (Wang & Buzsáki, 1996), Fig. S4, and, separately, the integrate-and-fire model adopted from (Vogels and Abbott, 2005, 2009), Fig S5. Both of these models exhibit Type 1 membrane excitability.

As in the main manuscript, for these simulations, we have kept inhibition constant and modified w_E and calculated total current as a function E/I ratio.

Wang-Buzsaki Model

Each neuron is described in the same form of three differential equations as the model neuron in the main manuscript, with different values of some parameters. The equation governing membrane voltage of the *i*-th cell is:

$$C\frac{dV_i}{dt} = -g_{Na}m_\infty^3(V_i)h(V_i - V_{Na}) - g_{Kdr}n^4(V_i - V_K) - g_L(V_i - V_L) + I_i^{drive} - I_i^{syn}$$

with $m_\infty = \frac{\alpha_m(V)}{\alpha_m(V)+\beta_m(V)}$, with $\alpha_m(V) = 0.1\frac{V+35}{1-\exp\left[-\frac{V+35}{10}\right]}$ and $\beta_m(V) = 4\exp[-\frac{u+60}{18}]$.

The gating equations are:

$$\frac{dh}{dt} = (h_\infty(V) - h)/\tau_h(V)$$

with $h_\infty(V) = \frac{\alpha_h(V)}{\alpha_h(V)+\beta_h(V)}$, $\tau_h(V) = \frac{0.2}{\alpha_h(V)+\beta_h(V)}$, where $\alpha_h(V) = 0.07\exp[\frac{-V-58.0}{20}]$, $\beta_h(V) = \{1 + \exp[\frac{-V-28}{10}]\}^{-1}$

and

$$\frac{dn}{dt} = (n_\infty(V) - n)/\tau_n(V)$$

with $n_\infty(V) = \frac{\alpha_n(V)}{\alpha_n(V)+\beta_n(V)}$, $\tau_n(V) = \frac{0.2}{\alpha_n(V)+\beta_n(V)}$, where $\alpha_n(V) = 0.01\frac{V+34}{1-\exp[-\frac{V+34}{10}]}$, $\beta_n(V) = 0.125\exp[-\frac{V+44}{80}]$.

Other parameters are $C = 1\mu F/cm^2$, $I_i^{drive} = 0.145\mu A$, g_{Na}=35.0 mS/cm^2, g_{Kdr}=9.0 mS/cm^2, V_{Na}=55.0mV, V_K=-90.0mV, and V_L=-65.0mV. g_L=0.1mS/cm^2.

The results (Fig. S4) are qualitatively the same as those presented in the main manuscript (Fig. 1b)

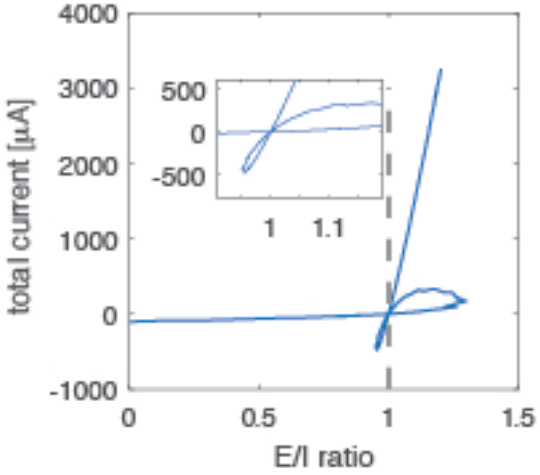

Figure S4. Total current plotted as a function of E/I ratio (both terms are defined in the main manuscript) for Buzsaki-Wank neuron model. As in the main manuscript we are changing implicitly the excitatory weight w_E. We observe non-monotonic changes in the E/I balance and the total current.

Integrate and fire model

The model was adopted from (Vogels and Abbott, 2005, 2009). Each neuron is described by the equation:

$$\tau \frac{dV}{dt} = (V_{rest} - V) + I_{ext} + I_{syn}.$$

Similarly, to that described in the manuscript, synaptic current transmitted from neuron j to neuron i at time t is given by $I_{ij}^{syn} = w \exp(-\frac{t-t_j}{\tau})(V_i - E_{syn})$, where t_j is the timing of the presynaptic spike in neuron j. Here, we have used the following parameters:

- Resting membrane potential (or reset potential) is set to -60mV
- Excitatory to excitatory connection strength, w_{EE}=[0.1, 0.49].
- Reversal potential for excitatory synapses $E_{syn}^{excitatory} = 0$,
- Firing threshold is set to -10.5mV
- Reversal potential for inhibitory synapses $E_{syn}^{inhibitory} = -80mV$
- Synaptic time constant of excitatory synapses $\tau = 5ms$,
- Synaptic time constant of inhibitory synapses $\tau = 10ms$,

Other parameters are as follows:

External depolarizing current of excitatory neurons I_{ext}	External depolarizing current of inhibitory neurons I_{ext}	Excitatory to inhibitory connection strength w_{EI}	Inhibitory to excitatory connection strength w_{IE}	Inhibitory to inhibitory connection strength w_{II}
$7 \pm 3mS$	$0 \pm 3mS$	0.5	1	0.2

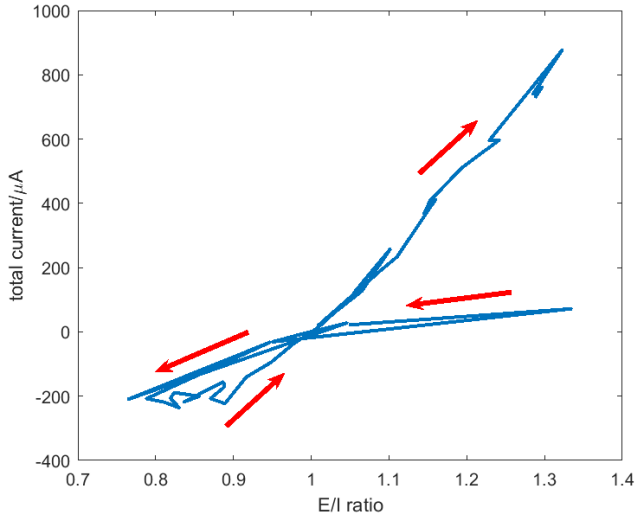

Figure S5. Total current plotted as a function of E/I ratio (both terms are defined in the main manuscript) for leaky integrate-and-fire model neuron model. As in the main manuscript we are changing implicitly the excitatory weight w_E. We observe non-monotonic changes in the E/I balance and the total current.

Qualitatively the results (i.e. loop formation) are the similar to those observed for other neuronal models indicating universality of the result.

References:

Wang XJ, Buzsáki G. Gamma Oscillation by Synaptic Inhibition in a Hippocampal Interneuronal Network Model. Journal of Neuroscience 1996;16(20) 6402-6413.

Vogels TP, Abbott LF. Signal propagation and logic gating in networks of integrate-and-fire neurons. Journal of neuroscience 2005; 25(46) 10786-10795.

Vogels TP, Abbott LF. Gating multiple signals through detailed balance of excitation and inhibition in spiking networks. Nature neuroscience 2009; 12(4) 483.